Photoionization of Be-like neon (Ne VII) from the low-lying states: Energies, widths, branching ratios, and oscillator strengths of the $1s$-$2p$ resonances

Jiaolong Zeng and Jianmin Yuan
Department of Applied Physics, National University of Defense Technology, Changsha 410073, People's Republic of China
(Received 14 April 2002; published 26 August 2002)

Seventeen-state close-coupling calculations are performed on the photoionization near the $1s$-$2p$ resonance region from the terms belonging to the configurations $1s^22s^2$, $1s^22s2p$, and $1s^22p^2$, of Be-like neon ions, Ne VII. The calculations include the total and partial photoionization cross sections and the contributions of the main ionization channels to the partial cross sections. The resonance energies, widths, and branching ratios of the $1s$-$2p$ core-excited states are determined from these cross sections. The resonance oscillator strengths of the corresponding $1s$-$2p$ transitions from Ne VII low-lying states are also obtained by integrating the photoionization cross sections. Our theoretical resonance energies, widths, and branching ratios are compared with existing experiments on the Auger spectra and other theoretical results. The calculated resonance energies are in rather good agreement with the latest experiment on the Auger spectra. For the autoionization width, good agreement is also found with recent theoretical results wherever available obtained using a saddle-point complex-rotation method.

DOI: 10.1103/PhysRevA.66.022715 PACS number(s): 32.80.Fb, 32.80.Hd, 32.80.Dz, 32.70.Cs

I. INTRODUCTION

Radiative data such as oscillator strengths and autoionization widths for the inner-shell transitions are of importance in laboratory and astrophysical plasmas. Recently, we [1,2] reported on the x-ray transmission and radiative opacity of laser-produced Al plasmas under local thermodynamic equilibrium by using the detailed-term-accounting (DTA) approximation. It was shown that the autoionization resonance widths of the excited states of a $1s$ electron being excited to $2p$ orbital are generally larger than the Stark and Doppler broadening under the prototype experimental conditions [3,4] and therefore becomes the major broadening mechanism. In simulating the x-ray transmission, one should take it into account in order to obtain better agreement with the experimental spectra. However, in the past years most calculations on the x-ray spectra had been carried out by only considering the Doppler broadening (for examples, see [5,6]). The autoionization resonance broadening had often been neglected, as is the case here on the Be-like complex Ne VII.

The present paper considers the photoionization and K-shell photoexcitation for the few low-lying states of Be-like Ne VII whose configurations belong to $2s^2$, $2s2p$, and $2p^2$. Attention is paid to determining the resonance energies and widths of the $1s$-$2p$ excited states by analyzing the resonance structures of the cross sections. The branching ratios and resonance oscillator strengths can also be obtained from the partial cross sections and the contributions of different ionization channels to the partial cross sections. Close-coupling calculations of the *K*-shell photoionization, which include the inner-shell resonances, have been restricted to relatively simple systems or lowly charged ions. For examples we have Li-like Li I [7–10] and C IV [11,12]; Be-like Be I [13], B II [14], and C III [11], B I [15]; O II, and O III [16]; O-like O I [17,18] and Ne III [19]; Ne I [20], Fe I [21,22], and Fe II [22]. For the highly charged ions, less work has been carried out. Recently, Bautista [23] calculated the photoionization cross sections of Fe XV from the first threshold to the *K*-shell thresholds. Gorczyca *et al.* [24] performed calculations of the photoabsorption cross section of Fe XV near the $2p^{-1}$ and $2s^{-1}$ edges within the framework of the *R*-matrix theory. We [25] investigated the photoionization for the ground state of Al VII from the threshold to the *K* shell. The resonances across the *L*-shell and *K*-shell thresholds are analyzed and the resonance energies and widths of some of the autoionization states are determined. For Ne ions, some work had been done on electron-impact excitation (for examples see [26,27]). Yamaoka *et al.* [28] experimentally investigated the photoionization of singly and doubly charged Ne ions near the *K*-shell ($1s$-$2p$) autoionizing resonance region in the 841–858 eV and 850–863 eV photon-energy range using a photon-ion merged-beam apparatus with an electron cyclotron resonance ion source. It is believed that this kind of experiment will be extended to highly charged Ne ions. For Ne VII ions, some experimental results on the $1s$ core-excited resonances from ion-atom collision experiments [29–31] have been reported in the literature. Recently, Lin *et al.* [32,33] and Shiu *et al.* [34] calculated the energies and Auger widths for some $1s$-$2p$ excited resonances ($1s2s^22p\,^{3,1}P^o$, $1s2s2p^2\,^{3,1}S$, $^{3,1}P$, $^{3,1}D$, and $1s2p^3\,^{1}P^o$) for the Be-like ions from Be to Ne VII using a saddle-point complex-rotation method. However, these investigations did not cover $1s2p^3\,^3P^o$, $^3D^o$, $^1D^o$ resonances.

The resonance energies, autoionization widths, branching ratios, and oscillator strengths of the $1s$-$2p$ excited states from the $n=2$ complex configurations of Ne VII are very useful in simulating the *K*-shell absorption spectra as well as being helpful for identifying the relevant Auger spectra. To access the accuracy of our theoretical data, we compare the calculated resonance energies with the experiments on the Auger spectra [29–31] and other theoretical results. The calculated autoionization widths and branching ratios are compared with recent theoretical results wherever available obtained by Lin *et al.* [32,33] and Shiu *et al.* [34] using a saddle-point complex-rotation method.

II. THEORETICAL METHODS

The photoionization cross sections are calculated by using the close-coupling approximation employing the *R*-matrix method [35,36]. The *R*-matrix method for electron-atom and photon-atom interactions has been discussed in great detail by Burke *et al.* [37]. It is very effective in considering the resonance structures, and especially, the autoionization resonance widths are naturally included in the calculations and can be determined [25,38,39]. In an *R*-matrix calculation, the wave function of the $N+1$ electron system is given the form

$$\Psi_k(X_1, \ldots, X_{N+1}) = \hat{A} \sum_{ij} c_{ijk} \Phi_i(X_1, \ldots, X_N, \hat{\mathbf{r}}_{N+1} \sigma_{N+1}) \times u_{ij}(r_{N+1}) + \sum_j d_{jk} \phi_j(X_1, \ldots, X_{N+1}), \quad (1)$$

where $\hat{A}$ is the antisymmetrization operator to take the exchange effect between the target electrons and the free electron into account. X_i stands for the spatial ($\mathbf{r}_i$) and the spin (σ_i) coordinates of the ith electron. The functions $u_{ij}(r)$ under the first sum construct the basis sets for the continuum wave functions of the free electron, and Φ_i are the coupling between the target states and the angular and spin part of the free electron. The correlation functions ϕ_j in the second sum are constructed by the square integrable orbitals to account for the correlation effects not adequately considered because of the cutoff in the first sum. The square integrable orbitals are cast as linear combinations of Slater-type orbitals

$$P_{nl}(r) = \sum_j C_{jnl} r^{I_{jnl}} \exp(-\xi_{jnl} r). \quad (2)$$

The parameters ξ_{jnl} and coefficients C_{jnl} are determined by a variational optimization on the energy of a particular state, whilst the powers of r (I_{jnl}) remain fixed.

For the calculations of the photoionization cross sections from the Ne VII low-lying states, ten real and four pseudo-orbitals ($1s$, $2s$, $2p$, $3s$, $3p$, $3d$, $4s$, $4p$, $4d$, $4f$, $\overline{5s}$, $\overline{5p}$, $\overline{5d}$, and $\overline{5f}$) are included in the wave-function expansion of the target Ne VIII ions. The pertinent parameters ξ_{jnl} and coefficients C_{jnl} for all orbitals are obtained by using the CIV3 code [40] according to the following rules. The $1s$ and $2s$ orbitals are the Hartree-Fock orbitals for the Ne VIII ground state $1s^2 2s\,^2S$ given by Clementi and Roetti [41], while the $2p$, $3s$, $3p$, $3d$ $4s$, $4p$, $4d$, and $4f$ orbitals are optimized on their respective terms of $1s^2 nl$ configuration, using the same $1s$ and $2s$ orbitals for each. The pseudo-orbitals $\overline{5s}$ are obtained by optimizing on the ground state of the Ne VIII $1s^2 2s\,^2S$ term, $\overline{5p}$ on the core-excited states $1s2s^2\ ^2S$, $\overline{5d}$ on the $1s2s2p\,^2P^o$ state, and $\overline{5f}$ on the $1s2p^2\,^2D$ state.

The appropriate *R*-matrix wave-function expansions are performed by including 17 terms of Ne VIII, in which eight core-excited states are included. The calculated energies relative to the ground state of Ne VIII are given in Table I, in which the unpublished NIST data (http://physics.nist.gov/cgi-bin/AtData/) are also given for comparison. It can be seen that the relative differences between our calculated data and NIST data are nearly 0.2% for the valence-electron excited states except for the $1s^2 2p\,^2P^o$ state. It is noted that all of the theoretical values show a similar deviation from the NIST data, indicating that the main source of inaccuracy is that the ground state is slightly too high in energy compared with the other valence-electron excited states. For the core-excited states, the differences are even smaller wherever the NIST data are available. The relative differences are 0.001% and 0.03%, respectively, for core-excited states $1s2s2p\,^2P^o$ and $1s2p^2\ ^2D$.

TABLE I. Calculated energies (in Ry) for the target Ne VIII ions relative to the ground state compared with the NIST data (http://physics.nist.gov/cgi-bin/AtData/).

State	NIST	This work	Diff.(%)
$(1s^2)2s\,^2S$	0.0	0.0	0.0%
$2p\,^2P^o$	1.17783	1.16927	0.73%
$3s\,^2S$	10.0227	10.0052	0.17%
$3p\,^2P^o$	10.3442	10.3243	0.19%
$3d\,^2D$	10.4563	10.4315	0.24%
$4s\,^2S$	13.3924	13.3695	0.17%
$4p\,^2P^o$	13.5236	13.5003	0.17%
$4d\,^2D$	13.5703	13.5447	0.19%
$4f\,^2F^o$	13.5724	13.5470	0.19%
$1s2s^2\,^2S$		65.5292	
$1s2s2p\,^4P^o$		65.8366	
$1s2s2p\,^2P^o$	66.7403	66.7412	0.001%
$1s2p^2\ ^4P$		67.0761	
$1s2s2p\,^2P^o$		67.1717	
$1s2p^2\ ^2D$	67.6497	64.6269	0.03%
$1s2p^2\ ^2P$		67.8221	
$1s2p^2\ ^2S$		68.4845	

In running the *R*-matrix codes, the *R*-matrix boundary is chosen to be 14 a.u. to ensure that the wave functions are completely wrapped within the *R*-matrix sphere. For each angular momentum, the continuum orbitals are expressed as a linear combination of 50 numerical basis functions. In order to take into account the resonances of *K*-shell excited states, only one electron is fixed in the $1s$ orbital, the other electrons can freely be distributed among the included orbitals.

III. RESULTS AND DISCUSSIONS

To have a general understanding of the photoionization of Ne VII ions, Fig. 1(a) displays the total photoionization cross sections of the ground state $1s^2 2s^2\,^1S$ from the first threshold to the *K* shell. Good agreement is obtained between the length and velocity forms of cross sections (the relative difference is less than 5.5%), thus only the length form is given. The ionization potentials (IP) obtained from the calculation of photoionization is 15.2162 Ry, differing from the experimental values 15.2345 Ry only by 0.12%. The resonance

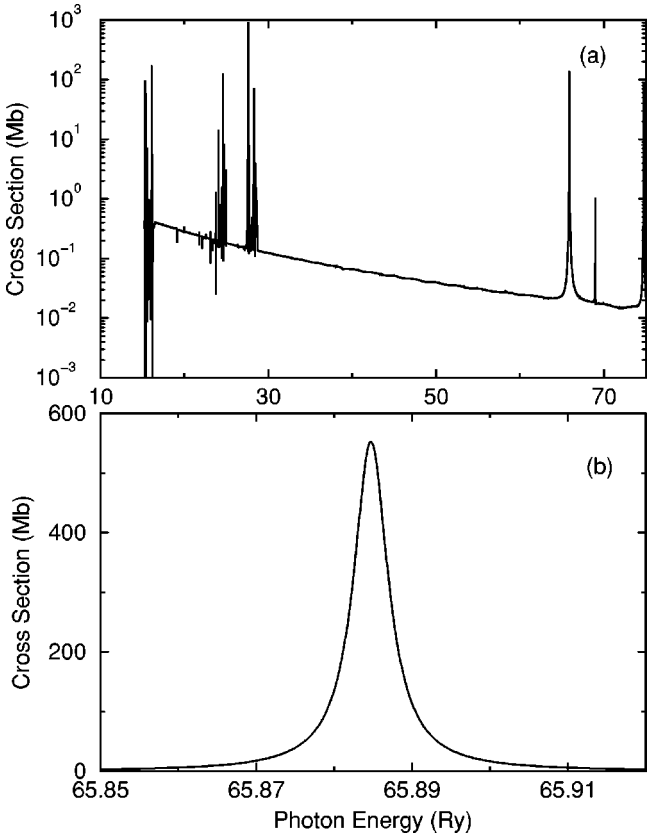

FIG. 1. (a) Ground-state photoionization cross section of Ne VII from the first ionization threshold to the *K*-shell thresholds, (b) the $1s$-$2p$ resonance in an expanded scale.

structures of the cross sections around the *L* shell at photon-energy ranges of about 15–30 Ry and the *K* shell above 65 Ry can easily be seen. The most striking feature of the cross sections is that a broad and strong resonance exists at 65.8847 Ry. This is the first *K*-shell resonance which should be assigned to be a $1s2s^22p\,^1P^o$ autoionization state. In the present work, we will not discuss the complex resonances around the *L* shell shown in the photon-energy range of 15–30 Ry, nor will we investigate the resonances around the *K*-shell thresholds which are above the $1s2s^22p\ ^1P^o$ resonance. In the following, we will only discuss the $1s$-$2p$ resonances in some details. Particularly in the case of *K*-shell resonances one would need to address the effects of Auger broadening, which we have neglected here.

In order to see clearly the $1s$-$2p$ resonance shown in Fig. 1(a), it is redrawn in Fig. 1(b) in an expanded scale. It can be seen that this resonance rises by up to orders of magnitude above the background and contributes significantly to the cross sections. The maximum caused by the $1s2s^22p\ ^1P^o$ resonance is about 550 Mb. When away from resonances, the cross sections are very small (0.1 Mb at 65.5670 Ry and decrease further to 0.05 Mb at 65.5437 Ry). This is a general feature for the $1s$-$2p$ resonances. By analyzing the resonance, one can determine the corresponding autoionization width. In the present work, the resonance positions and widths are obtained by fitting a Fano profile

$$\sigma=\sigma_a+\sigma_b\frac{(q+\varepsilon)^2}{1+\varepsilon^2}, \tag{3}$$

where σ_a and σ_b stand for constants related to the background and the resonance cross sections, respectively, $\varepsilon=2(E-E_0)/\Gamma$ with E being the photon energy, E_0 the resonance energy, and Γ the autoionization width, and the parameter q describes the shape of the resonance. By this way, the autoionization width of the core-excited state $1s2s^22p\,^1P^o$ is determined to be 72.1 meV.

The resonance oscillator strength of the corresponding $1s$-$2p$ transition can also be obtained from the photoionization cross sections. It is well known that the photoionization cross sections can be obtained from the differential oscillator strengths $df/d\epsilon$,

$$\sigma_{PI}=\frac{\pi he^2}{mc}\frac{df}{d\epsilon}=4\pi^2\alpha a_0^2\frac{df}{d\epsilon}, \tag{4}$$

where h is Planck's constant, e the electron charge, m the electron rest mass, c the speed of light in vacuum, and α and a_0 the fine-structure constant and the Bohr radius, respectively. In the latter expression of Eq. (4), ϵ is in Ry. The resonance oscillator strengths can be obtained from the photoionization cross sections σ_{PI},

$$f(L_iS_i\rightarrow L_jS_j)=\int_{\Delta E_r}\left(\frac{df(L_iS_i\rightarrow L_jS_j)}{d\epsilon}\right)d\epsilon$$
$$=\left(\frac{1}{4\pi^2\alpha a_0^2}\right)\int_{\Delta E_r}\sigma_{PI}(\epsilon;L_iS_i\rightarrow L_jS_j)d\epsilon, \tag{5}$$

where L_i, S_i, L_j, S_j are the total spin and orbital angular momenta of the initial bound level and the final continuum wave function, governed by the dipole selection rules. As the cross section σ_{PI} are usually calculated in length and velocity forms, the corresponding resonance oscillator strengths are determined in length f_l and velocity f_v forms as well. As has been pointed out above, the background cross sections are very small compared with the resonances, thus the contributions from the continuum cross sections are also very small. Using this method, we determine that the length and velocity forms of the $1s$-$2p$ transition $1s^22s^2\,^1S$–$1s2s^22p\,^1P^o$ are 0.5755 and 0.5617, respectively. The relative difference is only 2.4%.

Figures 2 and 3 display the total photoionization cross sections of the terms belonging to the configurations $(1s^2)2s2p$ and $2p^2$ in the vicinity of the $1s$-$2p$ resonances. In Fig. 2,(a) refers to the $2s2p\,^3P^o$ term and (b) to the $2s2p\,^1P^o$ term. In Fig. 3, (a) refers to the $2p^2\,^3P$ term, (b) to the $2p^2\,^1D$, and (c) to the $2p^2\,^1S$. The calculated energies of these terms relative to the ground state $1s^22s^2S$ of Ne VIII are given in Table II. For comparison, the unpublished data of Kelly [42] are also given. Good agreement is obtained between the calculated and the observed values, the relative differences being less than 0.2% for all of the six given terms. Table III shows the resonance energies and autoionization widths of the core-excited states and the resonance os-

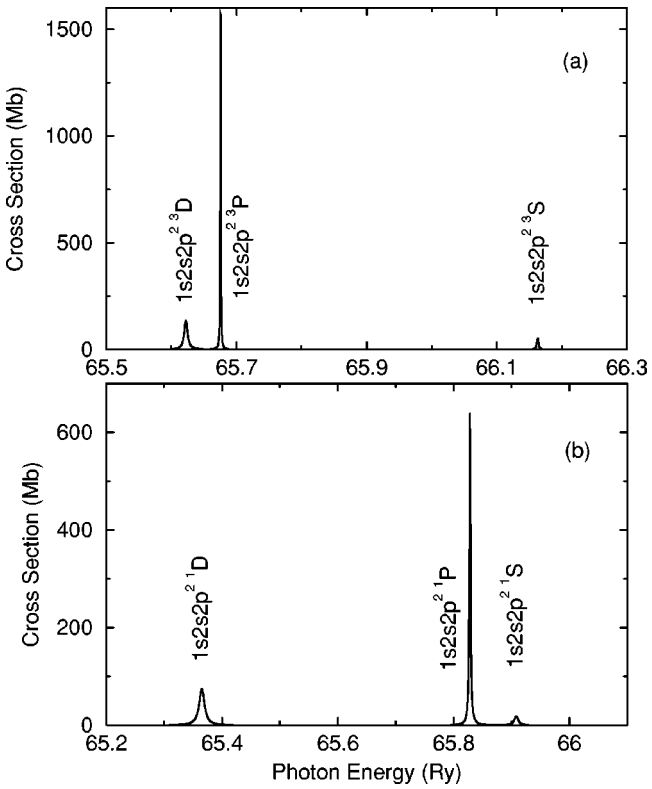

FIG. 2. Photoionization cross sections of the configuration $1s^2 2s 2p$: (a) $^3P^o$ and (b) $^1P^o$ in the vicinity of $1s$-$2p$ resonances.

cillator strengths of the corresponding $1s$-$2p$ transitions obtained from the present calculations. One can see that the energies of the $1s$-$2p$ transitions listed in Table III range from 65.3397 Ry for $1s^2 2p^2\,{}^3P - 1s 2p^3\,{}^3P^o$ to 66.1627 Ry for $1s^2 2s 2p\,{}^3P^o - 1s 2s 2p^2\,{}^3S$ (except for the three-electron excitation of $1s^2 2p^2\,{}^3P - 1s 2s^2 2p\,{}^3P^o$). Their average is about 65.7 Ry. They are well above the first ionization threshold 15.2345 Ry of Ne VII. The autoionization widths differ considerably for different core-excited states. The largest value is 146.9 meV for the state $1s 2s 2p^2\,{}^1D$ while the smallest is 11.8 meV for the state $1s 2s 2p^2\,{}^3P$. The largest is greater than the smallest by more than an order of magnitude. It is also noted that the widths of the singlet manifold are generally larger than those of corresponding triplet manifold. For example, the widths of the $1s 2s 2p^2\,{}^1D$ and ^3D states are 146.9 and 81.6 meV, respectively. It should be noted that the autoionization width of the $1s$-$2p$ excited states is larger than the Doppler and Stark widths under some typical plasma conditions, as we [39] have pointed out in our previous paper. This will make it more complicated for the modeling of the inner-shell x-ray absorption spectra of plasmas because one has to take the autoionization width into account.

From the inspection of Table III, one can see that rather good agreement is found between the length and velocity forms of the resonance oscillator strengths. The relative differences are less than 2.8% except for the weak three-electron transition $1s^2 2p^2\,{}^3P - 1s 2s^2 2p\,{}^3P^o$ (5.2%). The good agreement of the oscillator strengths between the

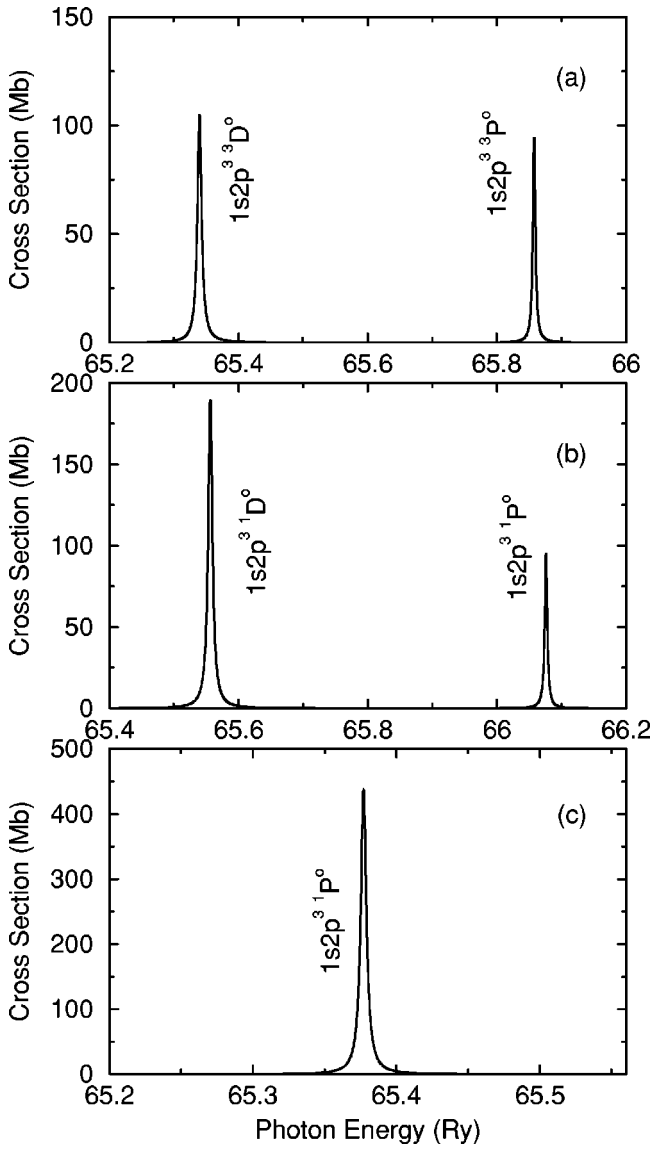

FIG. 3. The same as Fig. 2, but for the configuration $1s^2 2p^2$: (a) ^3P, (b) ^1D, and (c) ^1S terms.

length and velocity forms reflects the quality of the calculated photoionization cross sections in the vicinity of the $1s$-$2p$ resonance region. In the nonresonance region, good agreement is also found between the length and velocity

TABLE II. Comparison of the present calculated energies relative to the ground state $1s^2 2s^2 S$ of Ne VIII with the NIST data (http://physics.nist.gov/cgi-bin/AtData/) (in Ry) for the few low-lying terms of Ne VII.

Term	NIST	Calc.	NIST-Calc.	Diff.(%)
$2s^2\,{}^1S$	15.2345	15.2162	0.0183	0.12%
$2s 2p\,{}^3P^o$	14.2119	14.2015	0.0104	0.07%
$2s 2p\,{}^1P^o$	13.2757	13.2588	0.0169	0.13%
$2p^2\ {}^3P$	12.5893	12.5878	0.0015	0.01%
$2p^2\ {}^1D$	12.3210	12.3328	-0.0118	-0.10%
$2p^2\ {}^1S$	11.6058	11.6236	-0.0178	-0.15%

TABLE III. Resonance energy (E_r), autoionization width (Γ), length (f_l), and velocity (f_v) forms of the oscillator strengths of the $1s-2p$ transitions of Ne VII.

Transition	E_r (Ry)	Γ (meV)	f_l	f_v
$1s^22s^21S-1s2s^22p^1P^o$	65.8847	72.1	0.5746	0.5617
$1s^22s2p^3P^o-1s2s2p^23D$	65.6224	81.6	0.1601	0.1560
$1s^22s2p^3P^o-1s2s2p^23P$	65.6755	11.8	0.2799	0.2730
$1s^22s2p^3P^o-1s2s2p^23S$	66.1627	39.6	0.0305	0.0303
$1s^22s2p^1P^o-1s2s2p^21S$	65.9085	108.8	0.0297	0.0296
$1s^22s2p^1P^o-1s2s2p^21P$	65.8284	29.9	0.2911	0.2836
$1s^22s2p^1P^o-1s2s2p^21D$	65.3653	146.9	0.1563	0.1524
$1s^22p^23P-1s2s^22p^3P^o$	62.7533	98.0	0.0057	0.0054
$1s^22p^23P-1s2p^33P^o$	65.8580	63.9	0.0856	0.0848
$1s^22p^23P-1s2p^33D^o$	65.3397	105.4	0.1567	0.1526
$1s^22p^21D-1s2p^31P^o$	66.0763	61.2	0.0863	0.0854
$1s^22p^21D-1s2p^31D^o$	65.5564	104.8	0.2842	0.2769
$1s^22p^21S-1s2p^31P^o$	65.3672	62.6	0.3952	0.3842

forms of the photoionization cross sections (generally less than 2.5%).

As the $1s$-$2p$ core-excited states are autoionized ones, they can decay to different ionic states. In order to determine the branching ratios, we have obtained the partial photoionization cross section and the contributions of different ionization channels to the partial cross sections. For simplicity, these data are not presented here. The calculated branching ratios and Auger energies in eV to the main decay channels are presented in Table IV. Note that the branching ratios to the higher excited states are small and are not presented here. Therefore the sum of the given branching ratios for a particular core-excited states may not be necessarily equal to 100%. As we [25] have pointed out earlier, the resonance energy is closely related to the calculated ionization energy. Therefore, the Auger energies shown in Table IV have been corrected by the difference of the experimental (15.2345 Ry) and calculated (15.2162 Ry) first ionization potential. It can be seen that most core-excited states decay dominantly via some single channel. An earlier calculation carried out by Petrini [14] indicates that the *K*-shell excited state $1s2s^22p^1P^o$ of B II decay predominantly to the final excited ionic state B III $1s^22p$ rather than the ground state. This conclusion was later experimentally verified by Caldwell *et al.* [43] for the decay of Be $1s2s^22p^1P^o$ and it can be regarded as a common feature for the Be-like series. Following the work of Caldwell *et al.* [43], we calculate that the branching ratios of Ne VII $1s2s^22p^1P^o$ state to the channels $1s^22p+ks$ and $1s^22p+kd$ are 94.9% and 3.8%, respectively, while the branching ratio to the ground channel $1s^22s+kp$ is just 0.8%. Another example, the branching ratio of $1s2p^31D^o$ to the channel $1s^22p+kd$ is 99.8%. However, for some other core-excited states, they decay mainly via two channels. For example, the branching ratios of $1s2s2p^21D$ to channels $1s^22s+kd$ and $1s^22p+kp$ are 53.3% and 46.2%, respectively.

The data presented in this paper are useful to analyze experiments on photoionization as well as Auger spectra. Of course, the accuracy of our theoretical results need to be confirmed by the experiment. However, as far as we know, there are no experimental data on the *K*-shell photoionization of Ne VII in the literature for comparison. Fortunately, there are experiments on the Auger spectra which have determined the Auger energies and relative intensities of the Auger transitions. Table V gives the comparison of our calculated Auger energies obtained from the calculation of photoionization with the experimental and other theoretical results. Note that some of the identifications of the Auger spectra made by Bruch *et al.* [29] are tentative because of a lack of complete accurate theoretical data. It can be seen that good agreement is found between our calculated Auger energy and the experimental results of Bruch *et al.* [29] and the theoretical results of Lin *et al.* [32] and Shiu *et al.* [34]. Lin *et al.* [32] and Shiu *et al.* [34] reported the Auger widths and branching ratios of the core-excited states $1s2s^22p^3P^o$ and $1s2s2p^{2\,3,1}S$, $^{3,1}P$, $^{3,1}D$ for the Be-like isoelectronic sequence from Be to Ne VII using a saddle-point complex-rotation method. If the identification of the Auger spectra is correct then the agreement between our theoretical results

TABLE IV. Auger energy (E_{Auger}) (in eV) and branching ratios (BR) to the main decay channels for the Auger transitions of Be-like Ne VII ions obtained from the calculation of photoionization.

State	Channel	BR	E_{Auger}
$1s2s^22p^3P^o$	$1s^22s+kp$	33.9%	682.92
	$1s^22p+ks$	60.6%	667.01
	$1s^22p+kd$	4.9%	667.01
$1s2s^22p^1P^o$	$1s^22s+kp$	0.8%	689.63
	$1s^22p+ks$	94.9%	673.73
	$1s^22p+kd$	3.8%	673.73
$1s2s2p^23D$	$1s^22s+kd$	89.4%	699.87
	$1s^22p+kp$	10.2%	683.96
	$1s^22p+kf$	0.1%	683.96
$1s2s2p^23P$	$1s^22p+kp$	97.1%	684.68
	$1s^23p+kp$	0.3%	559.87
$1s2s2p^23S$	$1s^22s+ks$	77.6%	707.22
	$1s^22p+kp$	22.1%	691.31
$1s2s2p^21S$	$1s^22s+ks$	34.7%	716.59
	$1s^22p+kp$	64.4%	700.68
$1s2s2p^21P$	$1s^22p+kp$	98.8%	699.59
	$1s^23p+kp$	0.1%	575.03
$1s2s2p^21D$	$1s^22s+kd$	53.3%	709.20
	$1s^22p+kp$	46.2%	693.29
	$1s^22p+kf$	0.08%	693.29
$1s2p^33P^o$	$1s^22s+kp$	3.2%	725.03
	$1s^22p+ks$	14.5%	709.03
	$1s^22p+kd$	81.9%	709.03
$1s2p^33D^o$	$1s^22p+kd$	99.7%	702.07
	$1s^23p+kd$	0.2%	577.51
$1s2p^31P^o$	$1s^22s+kp$	0.7%	731.47
	$1s^22p+ks$	14.1%	715.56
	$1s^22p+kd$	84.7%	715.56
$1s2p^31D^o$	$1s^22p+kd$	99.8%	708.49
	$1s^23p+kd$	0.1%	583.93

TABLE V. Comparison of our calculated Auger energy in eV with the experimental and other theoretical results.

		Theory	
Auger transition	Expt.	Other work	This work
$1s2s^22p\,^3P^o-1s^22s+e^-$	683.2±0.1 [a]	683.30 [b]	682.92
	683±1 [c]	682.97 [d]	
	683.05(10) [e]	683.8 [c]	
$1s2s^22p\,^3P^o-1s^22p+e^-$	667.3±0.2 [a]	667.27 [b]	667.01
	666.88(1) [e]	666.95 [d]	
	665±1 [c]	667.83 [f]	
$1s2s2p^2\,^3D-1s^22s+e^-$	699.8±0.4 [a]	700.39 [b]	699.87
	702.00(13) [e]	700.24 [d]	
		701.42 [f]	
$1s2s2p^2\,^3D-1s^22p+e^-$	684.0±0.4 [a]	684.36 [b]	683.96
	686.64(5) [e]	683.99 [d]	
		684.4 [c]	
		685.28 [e]	
$1s2s2p^2\,^3P-1s^22p+e^-$	684.0±0.4 [a]	684.67 [b]	684.68
	684.05(7) [e]	684.28 [d]	
		684.57 [e]	
$1s2s2p^2\,^3S-1s^22s+e^-$		707.64 [b]	707.22
		707.60 [d]	
		708.47 [f]	
$1s2s2p^2\,^3S-1s^22p+e^-$	692.09(5) [e]	691.61 [b]	691.31
		691.575 [d]	
		692.34 [f]	
$1s2s^22p\,^1P^o-1s^22p+e^-$	673.8±0.2 [a]	674.17 [g]	673.73
	673.62(7) [e]		
$1s2s2p^2\,^1D-1s^22s+e^-$	710.0±0.4 [h]	709.46 [i]	709.20
		710.84 [a]	
		709.21 [h]	
$1s2s2p^2\,^1D-1s^22p+e^-$	694.0±0.4 [h]	693.43 [i]	693.29
	694.94(4) [e]	694.71 [a]	
		693.18 [h]	
$1s2s2p^2\,^1P-1s^22p+e^-$		699.64 [i]	699.59
		701.42 [a]	
$1s2s2p^2\,^1S-1s^22s+e^-$		716.71 [i]	716.59
		717.96 [a]	
		716.57 [h]	
$1s2s2p^2\,^1S-1s^22p+e^-$		700.68 [i]	700.68
		701.83 [a]	
		700.54 [h]	
$1s2p^3\,^3D^o-1s^22p+e^-$	703.65(18) [e]		702.07
$1s2p^3\,^1D^o-1s^22p+e^-$	709.34(4) [e]		708.49

[a]Reference [29].
[b]Saddle-point complex-rotation method, Ref. [32].
[c]Reference [31].
[d]$1/Z$ expansion, Ref. [29].
[e]Reference [30].
[f]Multiconfiguration Dirac-Fock calculations, Ref. [29].
[g]Reference [44].
[h]Reference [45].
[i]Saddle-point complex-rotation method, Ref. [34].

TABLE VI. Comparison of our calculated branching ratios to the main decay channels and autoionization width Γ with other theoretical results.

		Branching ratios		Γ (meV)	
State	Channel	This work	Other work	This work	Other work
$1s2s^22p\,^3P^o$	$1s^22s+kp$	33.9%	32.4% [a]	72.1	72.9 [a]
	$1s^22p+ks$	60.6%	64.4% [a]		
	$1s^22p+kd$	4.9%	3.2% [a]		
$1s2s2p^2\,^3D$	$1s^22s+kd$	89.4%	87.7% [a]	81.6	76.7 [a]
	$1s^22p+kp$	10.2%	12.3% [a]		
	$1s^22p+kf$	0.1%			
$1s2s2p^2\,^3P$	$1s^22p+kp$	97.1%	~100% [a]	11.8	11.4 [a]
	$1s^23p+kp$	0.3%			
$1s2s2p^2\,^3S$	$1s^22s+ks$	77.6%	76.2% [a]	39.6	39.2 [a]
	$1s^22p+kp$	22.1%	23.8% [a]		
$1s2s2p^2\,^1S$	$1s^22s+ks$	34.7%	30.38% [b]	108.8	
	$1s^22p+kp$	64.4%	69.62% [b]		
$1s2s2p^2\,^1P$	$1s^22p+kp$	98.8%	99.97% [b]	29.9	
	$1s^23p+kp$	0.1%			
$1s2s2p^2\,^1D$	$1s^22s+kd$	53.3%	47.73% [b]	146.9	
	$1s^22p+kp$	46.2%	58.27% [b]		
	$1s^22p+kf$	0.08%			

[a]Saddle-point complex-rotation method, Ref. [32].
[b]Saddle-point complex-rotation method, Ref. [34].

and the latest experiment carried out by Bruch *et al.* [29] is rather good. For examples, for the Auger transition $1s2s2p^2\,^3D-1s^22s+e^-$, our calculated Auger energy is 699.87 eV, in excellent agreement with the experimental value 699.8 ± 0.4 eV. Lin *et al.* [32] obtained a value of 700.39 eV, outside the experimental uncertainty. For $1s2s2p^2\,^3D-1s^22p+e^-$, our calculated energy is 683.96 eV, also in excellent agreement with the experimental value 684.0 ± 0.4 eV. For the Auger transition $1s2s^22p\,^1P^o-1s^22p+e^-$, the present theoretical value is 673.73 eV, again in excellent agreement with the experimental value 673.8 ± 0.2 eV. Shiu *et al.* [34] obtained a value of 674.17 eV, also outside the experimental uncertainty. From these examples it seems that present results should be rather accurate. In contrast, the experimental Auger energies obtained by Kádár *et al.* [30] are higher than the experimental results of Bruch *et al.* [29] and our theoretical results for $1s2s2p^2\,^3D-1s^22s+e^-$ [702.00(13) eV] and $1s2s2p^2\,^3D-1s^22p+e^-$ [686.64(5) eV]. While for transition $1s2s^22p\,^1P^o-1s^22p+e^-$, Kádár *et al.* [30] obtained a value of 673.62(7), in good agreement with the experimental results of Bruch *et al.* and our theoretical results.

Branching ratios and autoionization width are also of importance in analyzing resonances in photoionization process as well as in Auger spectra. Table VI gives the comparison of our calculated branching ratios and autoionization width with other theoretical results. From the inspection of Table VI, one can see that good agreement is found between our calculated autoionization width and the Auger width obtained by Lin *et al.* [32] using a saddle-point complex-rotation method. Good agreement is also found for the branching ratios, except for the core-excited state $1s2s2p^2\,^1D$. For this state, our result seems to be a reversion of the corresponding results obtained by Shiu *et al.* [34] for the two main ionization channels $1s^22s+kd$ and $1s^22p+kp$.

In summary, close-coupling calculations have been carried out to investigate the photoionization cross sections from the low-lying states of Be-like Ne VII ions. Emphasis is laid on analyzing the $1s-2p$ resonances and on obtaining the resonance energies, widths, and branching ratios of the core-excited states and the oscillator strengths of the $1s$-$2p$ transitions. The calculated resonance energies, autoionization widths, and branching ratios are compared with existing experimental and theoretical results on the Auger spectra. Rather good agreement is found between our results and other experimental and theoretical results. As present calculations cover all terms belonging to the $n=2$ complex configurations, we hope that they will be useful in future experiments on photoionization and on Auger spectra. However, it should be noted that present calculations do not include the effect of Auger broadening of resonances which is a general feature in the vicinity of the *K* edge. Therefore in comparing with future experiments such effects need to be included.

ACKNOWLEDGMENTS

This work was supported by the National Science Fund for distinguished Young scholars under Grant No. 10025416, the National Natural Science Foundation of China under Grant No. 19974075, the National High-Tech ICF Committee in China, and China Research Association of Atomic and Molecular Data.

[1] Jiaolong Zeng, Fengtao Jin, Jianmin Yuan, Qisheng Lu, and Yongsheng Sun, Phys. Rev. E **62**, 7251 (2000).
[2] Jiaolong Zeng, Jianmin Yuan, and Qisheng Lu, Phys. Rev. E **64**, 066412 (2001).
[3] S.J. Davidson, J.M. Foster, C.C. Smith, K.A. Warburton, and S.J. Rose, Appl. Phys. Lett. **52**, 847 (1988).
[4] T.S. Perry, S.J. Davidson, F.J.D. Serduke, D.R. Bach, C.C. Smith, J.M. Foster, R.J. Doyas, R.A. Ward, C.A. Iglesias, F.J. Rogers, J. Abdallah, Jr., R.E. Stewart, J.D. Kilkenny, and R.W. Lee, Phys. Rev. Lett. **67**, 3784 (1991).
[5] J. Jr. Abdallah and R.E.H. Clark, J. Appl. Phys. **69**, 23 (1991).
[6] C.A. Iglesias, J.K. Nash, M.H. Chen, and F.J. Rogers, J. Quant. Spectrosc. Radiat. Transf. **51**, 125 (1994).
[7] L. VoKy, P. Faucher, A. Hibbert, J.-M. Li, Y.-Z Qu, J. Yan, J.C. Chang, and F. Bely-Dubau, Phys. Rev. A **57**, 1045 (1998).
[8] L. VoKy, P. Faucher, H.L. Zhou, A. Hibbert, Y.-Z Qu, J.-M. Li, and F. Bely-Dubau, Phys. Rev. A **58**, 3688 (1998).
[9] H.L. Zhou, S.T. Manson, L. VoKy, P. Faucher, F. Bely-Dubau, A. Hibbert, S. Diehl, D. Cubaynes, J.-M. Bizau, L. Journel, and F.W. Wuilleumier, Phys. Rev. A **59**, 462 (1999).
[10] H.L. Zhou, S.T. Manson, P. Faucher, and L. VoKy, Phys. Rev. A **62**, 012707 (2000).
[11] D. Petrini and E.P. da Silva, Astron. Astrophys. **317**, 262 (1997).
[12] Jiaolong Zeng, Jianmin Yuan, Zengxiu Zhao, and Qisheng Lu, Eur. Phys. J. D **11**, 167 (2000).
[13] K.A. Berrington, J. Pelan, and L. Quigley, J. Phys. B **30**, 4973 (1997).
[14] D. Petrini, J. Phys. B **14**, 3839 (1981).
[15] N.R. Badnell, D. Petrini, and S. Stoica, J. Phys. B **30**, L665 (1997).
[16] D. Petrini and F.X. de Arujo, Astron. Astrophys. **282**, 315 (1994).
[17] B.M. McLaughlin and K.P. Kirby, J. Phys. B **31**, 4991 (1998).
[18] T.W. Gorczyca and B.M. McLaughlin, J. Phys. B **33**, L859 (2000).
[19] D. Petrini and G.A. Farias, Astron. Astrophys. **292**, 337 (1994).
[20] T.W. Gorczyca, Phys. Rev. A **61**, 024702 (2000).
[21] D.W. Donnelly, K.L. Bell, M.P. Scott, and F.P. Keenan, Astrophys. J. **531**, 1168 (2000).
[22] K.A. Berrington and C. Ballance, J. Phys. B **34**, L383 (2001).
[23] M.A. Bautista, J. Phys. B **33**, L419 (2000).
[24] T.W. Gorczyca, Z. Felfli, N.C. Deb, and A.Z. Msezane, Phys. Rev. A **63**, R010702 (2001).
[25] Jiaolong Zeng, Jianmin Yuan, and Qisheng Lu, Phys. Rev. A **64**, 042704 (2001).
[26] C.D. Griffin and Badnell, J. Phys. B **33**, 4389 (2000).
[27] D.M. Mitnik, D.C. Griffin, and N.R. Badnell, J. Phys. B **34**, 4455 (2001).
[28] H. Yamaoka, M. Oura, K. Kawatsura, T. Hayaishi, T. Sekioka, A. Agui, A. Yoshigoe, and F. Koike, Phys. Rev. A **65**, 012709 (2002).
[29] R. Bruch, D. Schneider, M.H. Chen, K.T. Chung, and B.F. Davis, Phys. Rev. A **44**, 5659 (1991).
[30] I. Kádár, S. Ricz, J. Végh, B. Sulik, D. Varga, and D. Berényi, Phys. Rev. A **41**, 3518 (1990).
[31] S. Schumann, K.O. Groeneveld, A. Nolte, and B. Fricke, Physica A **289**, 245 (1979).
[32] Shi-Hsin Lin, Chen-Shiung Hsue, and K.T. Chung, Phys. Rev. A **64**, 012709 (2001).
[33] Hsin Lin, Chen-Shiung Hsue, and K.T. Chung, Phys. Rev. A **65**, 032706 (2002).
[34] Wei Cheng Shiu, Chen-Shiung Hsue, and K.T. Chung, Phys. Rev. A **64**, 022714 (2001).
[35] K.A. Berrington, W.B. Eissner, and P.H. Norrington, Comput. Phys. Commun. **92**, 290 (1995).
[36] P.G. Burke and K.A. Berrington, *Atomic and Molecular Processes: An R-matrix Approach* (IOP Publishing, Bristol, 1993).
[37] P.G. Burke, A. Hibbert, and W.D. Robb, J. Phys. B **4**, 153 (1971).
[38] Jiaolong Zeng, Jianmin Yuan, and Qisheng Lu, Phys. Rev. A **62**, 022713 (2000).
[39] Jiaolong Zeng, Jianmin Yuan, and Qisheng Lu, J. Phys. B **34**, 2823 (2001).
[40] A. Hibbert, Comput. Phys. Commun. **9**, 141 (1975).
[41] E. Clementi and C. Roetti, At. Data Nucl. Data Tables **14**, 177 (1974).
[42] R.L. Kelly, http://physics.nist.gov/cgi-bin/AtData/.
[43] C.D. Caldwell, M.G. Flemming, M.O. Krause, P. van der Meulen, Cheng Pan, and A.F. Starace, Phys. Rev. A **41**, 542 (1990).
[44] M.H. Chen and B. Craseman, At. Data Nucl. Data Tables **38**, 381 (1988).
[45] A. Itoh, D. Schneider, T. Schneider, T.J.M. Zouros, G. Nolte, G. Schiwietz, W. Zeitz, and N. Stolterfoht, Phys. Rev. A **31**, 684 (1985).